Visual Neuroscience (2002), **19**, 39–49. Printed in the USA.

DOI: 10.1017.S0952523801191042

Optical imaging of orientation and ocular dominance maps in area 17 of cats with convergent strabismus

RALF ENGELMANN, JOHN M. CROOK, AND SIEGRID LÖWEL
Leibniz-Institut für Neurobiologie, D-39118 Magdeburg, Germany

(RECEIVED August 20, 2001; ACCEPTED December 10, 2001)

Abstract

Strabismus (or squint) is both a well-established model for developmental plasticity of the brain and a frequent clinical symptom. While the layout and topographic relationship of functional domains in area 17 of divergently squinting cats has been analyzed extensively in recent years (e.g. Löwel et al., 1998), functional maps in convergently squinting animals have so far not been visualized with comparable detail. We have therefore investigated the functional organization of area 17 in adult cats with a surgically induced convergent squint angle. In these animals, visual acuity was determined by both behavioral tests and recordings of visual evoked potentials, and animals with comparable acuities in both eyes were selected for further experiments. The functional layout of area 17 was visualized using optical imaging of intrinsic signals. Monocular iso-orientation domains had a patchy appearance and their layout was different for left and right eye stimulation, so that segregated ocular dominance domains could be visualized. Iso-orientation domains exhibited a pinwheel-like organization, as previously described for normal and divergently squinting cats. Mean pinwheel density was the same in the experimental and control animals (3.4 pinwheel centers per mm^2 cortical surface), but significantly ($P < 0.00001$) higher than that reported previously for normal and divergently squinting cats ($2.7/mm^2$). A comparison of orientation with ocular dominance maps revealed that iso-orientation domains were continuous across the borders of ocular dominance domains and tended to intersect these borders at steep angles. However, in contrast to previous reports in normally raised cats, orientation pinwheel centers showed no consistent topographical relationship to the peaks of ocular dominance domains. Taken together, these observations indicate an overall similarity between the functional layout of orientation and ocular dominance maps in area 17 of convergently and divergently squinting cats. The higher pinwheel densities compared with previous reports suggest that animals from different gene pools might generally differ in this parameter and therefore also in the space constants of their cortical orientation maps.

Keywords: Cat, Visual cortex, Functional domains, Optical imaging, Squint, Esotropia

Introduction

Strabismus (or squint) is the most common developmental disorder of the visual system. In strabismics, the visual axes do not meet at the fixation point but instead they converge (esotropia) or diverge (exotropia) causing double vision (diplopia). The visual system employs different strategies to avoid double vision: either the signals from one eye are chronically suppressed and thus excluded from conscious experience, or fixation occurs in an alternating mode, with both eyes participating at different moments in time (Duke-Elder & Wybar, 1973; von Noorden, 1990). Misalignment of the visual axes in early childhood leads to profound and often irreversible restrictions of adult visual performance. The visual acuity of the deviating eye is often dramatically reduced (strabismic amblyopia), and binocular functions, especially stereopsis, are reduced or not developed at all (stereo blindness).

Strabismus is also a well-established model for developmental plasticity in the visual cortex, because it is not actually the eyes that suffer but the cortex (Blakemore, 1976; Maffei & Bisti, 1976). The various forms of squint (convergent, divergent, with or without amblyopia) are accompanied by different psychophysical deficits (Duke-Elder & Wybar, 1973; Kalil et al., 1984; von Noorden, 1990) that may be due to modifications to the underlying functional architecture of the visual system. In the past, the layout and topographic relationships of functional domains in area 17 of divergently squinting cats have been analyzed in detail (Löwel, 1994; Löwel et al. 1998). It was shown that maps of orientation preference are not obviously modified by the artificial decorrelation of binocular input, although ocular dominance domains are clearly segregated (Shatz et al., 1977; Löwel, 1994). Additionally, in divergently squinting cats, horizontal intracortical connections between neurons activated *via* stimulation through different eyes

Address correspondence and reprint requests to: Siegrid Löwel, Leibniz-Institut für Neurobiologie, Forschergruppe "Visuelle Entwicklung und Plastizität", Brenneckestrasse 6, D-39118 Magdeburg, Germany. E-mail loewel@ifn-magdeburg.de. http://www.ifn-magdeburg.de/resgroups/rg4/rg4_home.jsp

are dramatically reduced (Löwel & Singer, 1992), and responses between neurons located in different ocular dominance domains are no longer synchronized (König et al., 1993).

While the optical axes of the eyes never cross with divergent squint, they do at a certain point in visual space with convergent squint. This creates very complex topological relationships of near/far and out of focus objects. Furthermore, callosal interhemispheric transfer is expanded in convergent squinters compared with normal cats and this is accompanied by reduced binocularity and orientation selectivity of cortical cells (Milleret & Houzel, 2001). Consequently, compensation strategies in convergent squinters might be more diverse, leading to an increased occurrence of amblyopia, myopia, or anomalous retinal correspondence (Grant & Berman, 1991) in addition to the common alternating fixation (von Grünau & Rauschecker, 1983; Tieman & Tumosa, 1997). We have therefore made a careful analysis of the visual capacities of our convergently squinting animals, using behavioral tests and recordings of visual evoked potentials (VEPs) to determine the visual acuities of both eyes. In the present study, we have used optical imaging of intrinsic signals to investigate the functional organization of area 17 in convergently squinting animals with comparable visual acuities in both eyes. Some of the results have been reported in abstract form (Engelmann et al., 1999).

Materials and methods

Twelve kittens from ten different litters (S1/S2 and S3/S6 were siblings) of the colony of the Leibniz-Institut für Neurobiologie in Magdeburg were included in the present study. In eight of the kittens (S1–S8), a convergent squint angle was induced surgically (Crewther et al., 1985; Sireteanu et al., 1993; Roelfsema et al., 1994) at the age of 17–21 days. Four normally raised cats (N1–N4) served as control animals. At the age of 4–8 months, visual acuity of both eyes was determined by behavioral testing (see Katz & Sireteanu, 1992; Cleland et al., 1982; Crewther et al., 1985; Roelfsema et al., 1994) using a modified jumping stand (the animals had to discriminate between square-wave gratings and equiluminant grey). Animals with comparable grating acuities in both eyes (difference <0.5 octave) were selected for further experiments. To complement the behavioral tests, we recorded VEPs in four of the strabismic cats (S4–S6, & S8).

After completion of the behavioral tests and VEP recordings, the layout of area 17 was determined using optical imaging of intrinsic signals (see Löwel et al., 1998) in all strabismic and two normally raised control cats. At the time of the optical-imaging experiments, the animals varied in age between 8 months and 3 years. Cortical activity maps were recorded while the animals were stimulated monocularly with moving gratings of different orientations. Intrinsic signal imaging exploits the fact that active cortical regions consume oxygen thereby accumulating deoxyhaemoglobin. Because deoxyhaemoglobin (compared with oxyhaemoglobin) absorbs more of the red light used to illuminate the cortex, active regions appear dark on the images (Blasdel & Salama, 1986; Grinvald et al., 1986; for a review see Bonhoeffer & Grinvald, 1996).

Squint induction

Anesthesia was induced with an intramuscular injection of ketamine hydrochloride (10 mg/kg, Ketanest®, Parke-Davis, Berlin, Germany) and xylazine hydrochloride (2.5 mg/kg, Rompun®, Bayer AG, Leverkusen, Germany). After incision of the conjunctiva, the tendon of the lateral rectus muscle was located and cut. In all animals, the angle of the resulting convergent squint was determined repeatedly during development using the corneal reflex method (Sherman, 1972; Olson & Freeman, 1978; von Grünau, 1979). The animals were manually restrained, several flashlight snapshots of the cat's head were taken, and the ratio of the distance between the corneal reflexes over the distance between pupils was determined on the photoprints. This ratio is a reliable indicator of eye alignment (Sherman, 1972; Sireteanu et al., 1993). The ratios of our experimental animals were always above 1.02 (1.02–1.05) and thus in the range for convergent squinters throughout the critical period (see Sireteanu et al., 1993; von Grünau, 1979).

Behavioral testing

Animals were trained to discriminate between a square-wave grating and equiluminant grey (Teller acuity cards, with a contrast of 82–84% and a luminance of 10 cd/m^2) on a modified jumping stand (Mitchell et al., 1976; Katz & Sireteanu, 1992). Jumps to the grating were rewarded (correct response). When the animals jumped correctly to gratings of moderate spatial frequencies, the test phase was started. The cats were tested monocularly through the normal and deviating eyes on alternate days, the other eye being occluded with a black contact lens during testing. Each eye was tested on at least five different days (for 50 trials per day or until the cat stopped jumping spontaneously). Five animals (S1–S3, S6, & S7) were tested with the method of constant stimuli (procedure I), in which 5–7 spatial frequencies ranging from 0.6 cycle/deg to 4.9 cycle/deg (0.5 octave intervals) were presented in random order. In another three strabismic cats (S4, S5, & S8), the spatial frequency of the cards was continuously adjusted to the performance of the animal (procedure II; Cleland et al., 1982). The spatial frequencies of the gratings ranged from 0.6 cycle/deg to 3.6 cycle/deg (0.5 octave intervals). After more than one incorrect response in a series of five jumps, the spatial frequency was reduced by two steps. After a correct response it was increased by one step. For each eye a minimum of 180 jumps were obtained. The resulting psychometric functions were interpreted such that the spatial frequency at which the animal performed at the 75% level was taken as the discrimination threshold. Animals were considered to be nonamblyopic if their interocular visual acuities differed by less than 0.5 octave. To evaluate naturally occuring interocular differences in visual acuity, two normally raised control cats (N3 & N4) were also examined in the jumping stand (procedure II).

VEP recordings

After completion of the behavioral tests, VEPs were recorded in four of the squinting animals (S4–S6 & S8). Silver ball electrodes of 1-mm diameter were positioned on the exposed dura above area 17 of either hemisphere (see Yin et al., 1994). The two electrodes were connected together and the common signal was recorded against an indifferent electrode in the neck muscles or attached to the optical imaging chamber. The stimulus consisted of two phase reversals of a high-contrast (80%) vertical square-wave grating (80 × 60 deg) separated by 700 ms. Steady-state VEPs were averaged from 50 stimulus pairs presented with an interstimulus interval of 2 s to either eye. Gratings of 6–8 different spatial frequencies ranging from 0.15 cycle/deg to 3.4 cycle/deg were presented in pseudorandom order. Signals were amplified (4600×), band-pass filtered (10–300 Hz), and sampled at a rate of 690 Hz.

Stimuli were generated by a "Leonardo" Visual Stimulus Generator (Lohmann Research Equipment, Duisburg, Germany), presented on an Iiyama Vision Master 502 21-inch monitor (background luminance 1.3 cd/m^2; refresh rate 85 Hz; resolution 800 × 600 pixel), and viewed *via* corrective corneal contact lenses with 3-mm-diameter artificial pupils at a distance of 28-cm. Data acquisition and analysis were performed using Spike2 software (Cambridge Electronic Design; CED, Cambridge, UK). Stimulus presentation and data acquisition were controlled by a CED-1401-Plus Interface.

Optical imaging

Surgery

Anesthesia was induced as described above (ketamine and xylazine hydrochloride) and maintained throughout the experiment using halothane/N_2O/O_2 anesthesia (70% N_2O/30% O_2, supplemented with 0.8–1.2% halothane, Eurim Pharma, Germany). The ECG, pulmonary pressure, end-tidal CO_2 (3–4%), and rectal temperature (37–38°C) were continuously monitored. The animal's head was fixed in a stereotaxic frame by means of a metal nut cemented to the skull. A craniotomy was performed over area 17 centered at Horsley-Clarke coordinate P4, and a stainless-steel chamber was implanted over the exposed cortical region with dental cement. After removing the dura, the chamber was filled with silicone oil and sealed with a round glass coverslip.

Visual stimulation

Animals were stimulated monocularly with high-contrast square-wave gratings (subtending 80 × 60 deg) of four equally spaced orientations (0, 45, 90, and 135 deg) moving at a speed of 4 deg/s. Spatial frequency (0.3–0.5 cycle/deg) was well below the animals' behavioral threshold. Stimuli were generated by EZV-Stim software (Optical Imaging Inc., Rehovot, Israel) and presented on an Iiyama Vision Master 502 monitor (parameters as for VEP recordings) at a distance of 28 cm. Eyes were refracted appropriately using contact lenses with artificial pupils of 3 mm.

Data acquisition

The cortical surface was illuminated by means of two adjustable light guides attached to a tungsten-halogen lamp (Spindler & Hoyer, Göttingen) equipped with interference filters for different wavelengths. The vascular pattern of the cortex was visualized at 546 ± 10 nm (green), cortical activity maps at 707 ± 10 nm (red). During data acquisition of intrinsic signals, the camera was focused 500–700 μm below the cortical surface. The ORA 2001 system (Optical Imaging Inc.), equipped with a cooled Theta CCD system (384 × 288 pixel chip from Thomson-CSF), was used for collecting the intrinsic signals. The camera acquired a series of frames every 12 s, whereby a grating of a given orientation and spatial frequency was presented for 2 s in static mode, followed by 3 to 4.2 s of data acquisition (5–7 frames of 600-ms duration) during which the grating was moved in both directions along the axis orthogonal to its orientation.

Data analysis

We first calculated "single condition maps" in which the images acquired during presentation of a particular stimulus were divided by the sum of all different stimulus conditions ("cocktail blank procedure"; see Bonhoeffer & Grinvald, 1993, 1996; Löwel et al., 1998). Ocular dominance maps were calculated by summing all monocular activity maps divided by the sum of all different stimulus conditions. For a comprehensive analysis of the organization of iso-orientation domains, the single responses to all different stimulus conditions were summed vectorially on a pixel-by-pixel basis. In the present analyses, the angle of the resulting vector is displayed and color-coded ("angle" map; see Bonhoeffer & Grinvald, 1996), so that the respective colors indicate the preferred orientation for this piece of cortex ("orientation preference map").

To characterize the local geometric relationship between iso-orientation domains and ocular dominance borders, we analyzed the statistics of their intersection angles as described in detail elsewhere (Löwel et al., 1998). To quantify the frequency of intersection angles, they were categorized into six classes of 15 deg ranging from 0 deg to 90 deg. As illustrated in Fig. 8 (left column), a preponderance of angles between 75 and 90 deg was observed. To exclude the possibility that this tendency for orthogonal intersections was accidental, we redetermined intersection angles after shifting the two maps from the same animal in increments of 10 pixels in both x and y directions (Fig. 8, right column).

The location and density of orientation pinwheel centers was determined as described in detail elsewhere (Löwel et al., 1998). Only orientation-preference maps that were of sufficient quality to unambiguously determine pinwheel centers were subjected to this analysis (7 hemispheres from 5 animals). Briefly, pinwheel centers were determined as the crossings of the 0 deg/90 deg with the 45 deg/135 deg orientation contours. Furthermore, we checked for every single point whether it represented a genuine orientation center in the corresponding angle maps. Points around which iso-orientation domains did not exhibit a clear radial organization were discarded from further analyzes. For analyzing pinwheel location with respect to ocular dominance borders, the relative frequency of pinwheel centers in different subregions of ocular-dominance maps was calculated using recently introduced approaches (Hübener et al., 1997; Löwel et al., 1998; Matsuda et al., 2000): those 10% of the pixels in an ocular dominance map with the highest values were defined as corresponding to the centers of the columns of one eye, whereas the 10% with the lowest pixel values defined the centers of the ocular dominance columns of the other eye.

Results

Visual acuity

The effects of the misalignment of the optical axes on visual acuity were determined psychophysically in eight cats (see Materials and methods). The threshold acuities of our convergently squinting cats as assessed in the jumping stand apparatus ranged from 1.7 cycle/deg to 2.9 cycle/deg (mean 2.4 cycle/deg) in the normal (left) and from 1.5 cycle/deg to 2.9 cycle/deg (mean 2.1 cycle/deg) in the deviating (right) eye (see Table 1). Examples of the cats' performance are illustrated in Fig. 1. Animals with comparable acuities in both eyes were selected for further experiments: in the present sample, mean acuity differences between the eyes were always below 0.3 cycle/deg and below 0.33 octave. To gain an impression of the natural variation of interocular acuity differences, we tested two normally raised control animals in the same jumping stand apparatus. The interocular difference in visual acu-

Table 1. *Visual acuities of esotropic (S1–S8) and normally raised cats (N3–N4)*[a]

Cat	Age (months)	Visual acuity (L/R)
S1	7	2.9/2.9
S2	8	1.7/1.5
S3	5	2.3/1.9
S4	4	1.8/1.5
S5	6	1.8/1.8
S6	7	2.4/2.0
S7	6	2.4/2.3
S8	7	2.5/2.1
N3	11	2.1/1.5
N4	10	2.5/1.5

[a]Shown is the visual acuity (cycle/deg) of the left (L) and right (R) eye, as assessed by behavioral testing. Age: age at the time of acuity test.

ity in these animals was 0.45 and 0.75 octave, respectively, and thus actually somewhat larger than that shown by our strabismic cats (see Table 1).

In some animals, the behavioral analyzes were complemented by recordings of VEPs (see Fig. 2). The VEP data confirmed the small interocular acuity differences of the animals that had been classified as nonamblyopic on the basis of behavioral testing.

Taken together, all animals selected for the optical-imaging experiments had a clear convergent squint angle throughout the critical period, behaviorally and electrophysiologically confirmed similar acuities in both eyes, and normal overall spatial-frequency selectivity (see also Roelfsema et al., 1994; Sireteanu et al., 1993).

Optical imaging

Using optical imaging of intrinsic signals, we recorded activity maps in area 17 of convergently squinting cats in 3.6 mm x 4.8 mm large regions in the central visual field representation at the junction of the lateral to the posterolateral gyrus of the brain (both ipsilateral and contralateral to the squinting eye). Examples of the blood-vessel pattern of the imaged cortical areas are illustrated in Figs. 3–6. Importantly, all animals were adult (>6 months of age) at the time of the imaging experiments.

Layout of ocular dominance domains

As described previously for divergently squinting cats (Löwel et al., 1998), monocular stimulation of convergently squinting cats with contours of a single orientation gave rise to activity patterns consisting of rather isolated patches (Fig. 3). In the esotropic animals, the layout of orientation domains activated through the right and the left eye clearly differed (compare left and right columns in Fig. 3), and ocular dominance domains could be readily visualized (Fig. 4). Specifically, ocular dominance domains in convergently squinting cats were complementary and clearly segregated: regions activated by the left eye in cat S1 (dark grey to black in Fig. 4b) appeared almost inactive with stimulation of the right eye (light grey to white in Fig. 4d). Another example of the complementarity of left- and right-eye domains in the strabismic cats is illustrated in Figs. 4e–4h. This is in contrast to

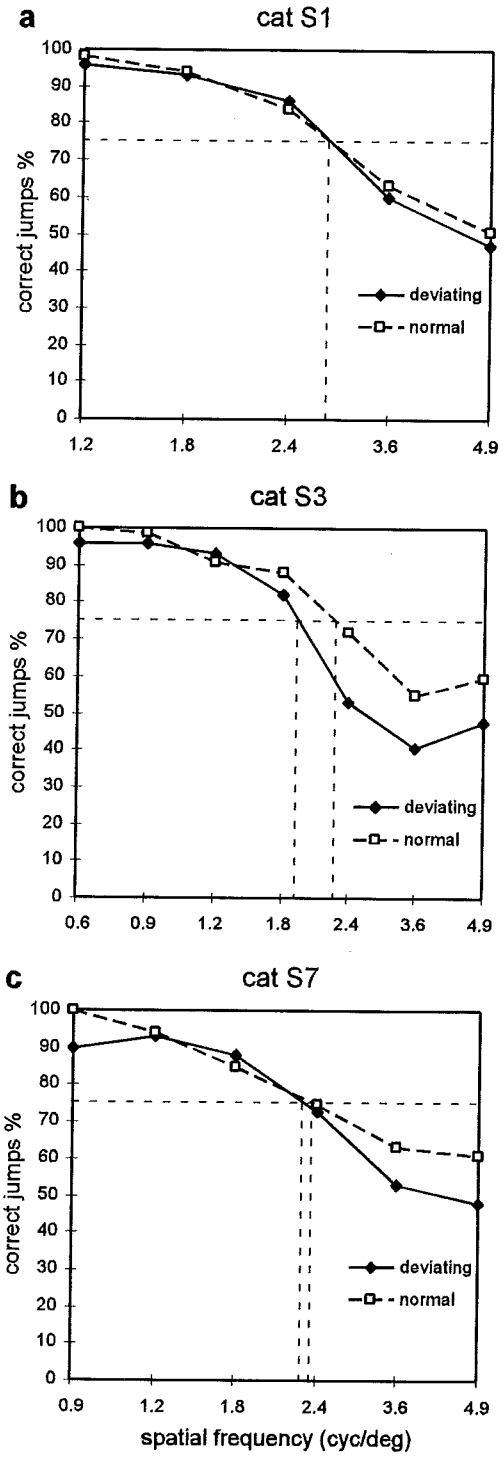

Fig. 1. Examples of behaviorally determined visual grating acuity of the normal (left) eye (white squares) and the deviating (right) eye (black diamonds) of cats S1 (a), S3 (b), and S7 (c). Tests were done in a modified jumping stand with standard Teller acuity cards. *X*-axis, spatial frequency of the test gratings in cycles/degree (cyc/deg). *Y*-axis, percentage of correct jumps made by the animals in the jumping stand apparatus. The horizontal (dashed) line indicates a 75% level of performance which was taken as the criterion for the discrimination threshold. Threshold acuities for the normal and deviating eye were 2.9 and 2.9 cyc/deg in cat S1, 2.3 and 1.9 cyc/deg in cat S3, and 2.4 and 2.3 cyc/deg in cat S7 (vertical dashed lines). Note that in all three cases visual acuity was similar in both eyes, with an interocular acuity difference of less than 0.25 octave. The cats were therefore classified as nonamblyopic convergent squinters.

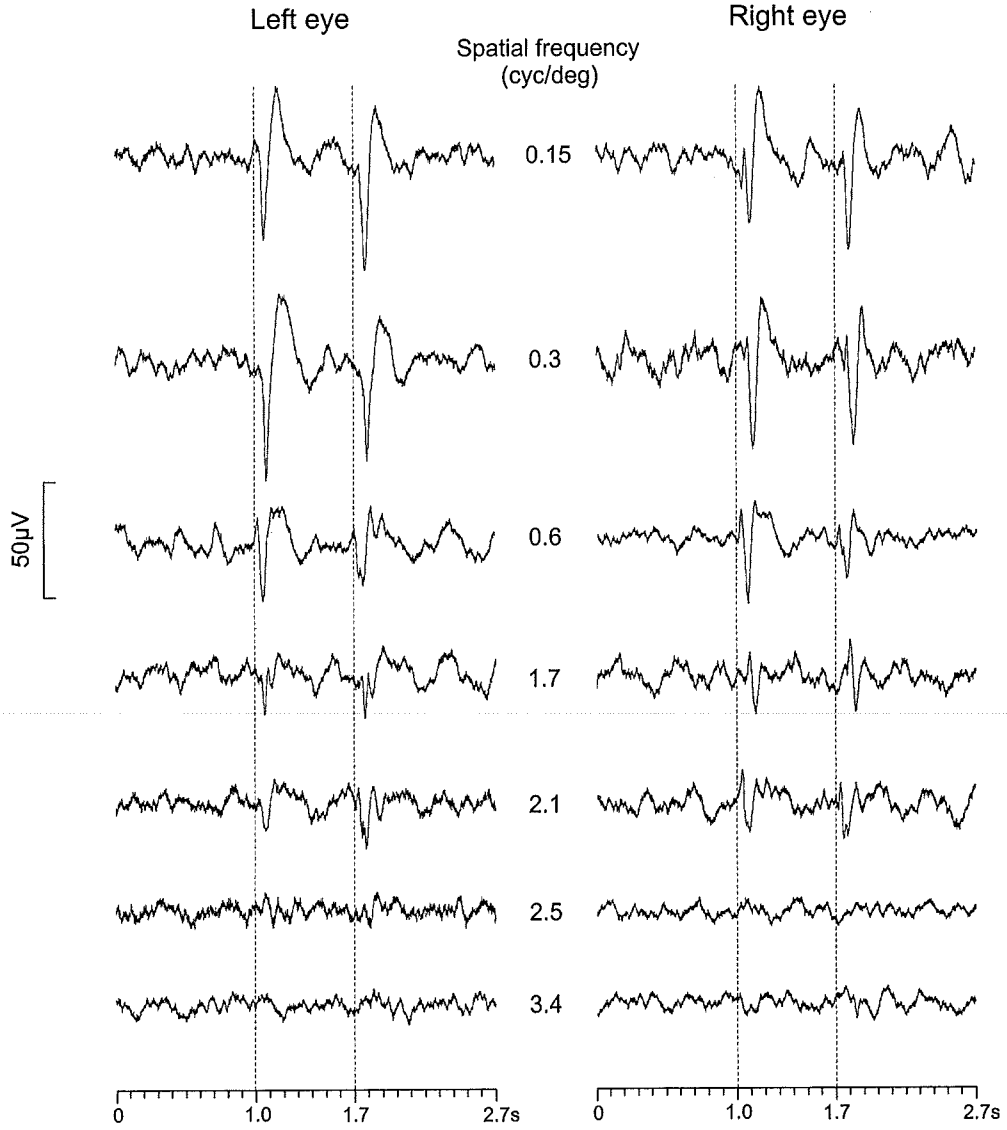

Fig. 2. Averaged VEPs (50 repetitions) from area 17 of convergently squinting cat S8 elicited by phase reversals of a square-wave grating. Vertical broken lines indicate the onset of each phase reversal at 1.0 and 1.7 s; each division on the *X*-axis represents 100 ms; *Y*-axis relative response. Left (normal) and right (deviating) eye responses are shown in left and right columns, respectively; spatial frequency indicated between the left and right eye responses. Note that the amplitude of the VEPs recorded through each eye was similar at all tested spatial frequencies and that the cutoff spatial frequency was also similar for each eye.

the situation in normally raised cats, in which the visualization of ocular dominance domains becomes increasingly difficult after a few weeks of life (Crair et al., 1997*a*; Hübener et al., 1997) because maps induced by stimulation through the two eyes become nearly identical (Crair et al., 1998). In Fig. 5, this is illustrated for one of our normally raised control animals (N1) in which activity patterns after left and right eye stimulation were similar (compare left and right columns of Fig. 5). Nevertheless, since activity patterns after left and right eye stimulation differed slightly, we were able to delineate ocular dominance domains in this normally raised animal (Fig. 6). The "contrast" of the ocular dominance map was, however, much weaker than in all strabismic cats: regions maximally activated by the left eye in cat N1 (dark grey in Fig. 6b) are also activated by the right eye (light grey in Fig. 6d). Importantly, there were no differences in activity levels between domains activated by the normal and deviating eye. Our optical imaging data thus gave no indication of a disadvantage of the deviating compared with the nondeviating eye in convergently squinting cats (Figs. 3 & 4), in line with recent observations in divergently squinting cats (Löwel et al., 1998).

Layout of orientation domains

As illustrated in Fig. 7, in both our convergently squinting (7a & 7e) and normally raised cats (Figs. 7b & 7c), iso-orientation domains exhibited a pinwheel-like organization as has been described previously for normally raised (e.g. Bonhoeffer et al., 1995) and divergently squinting cats (Löwel et al., 1998). The overall layout of orientation-preference maps was also similar in the experimental and normally raised control animals.

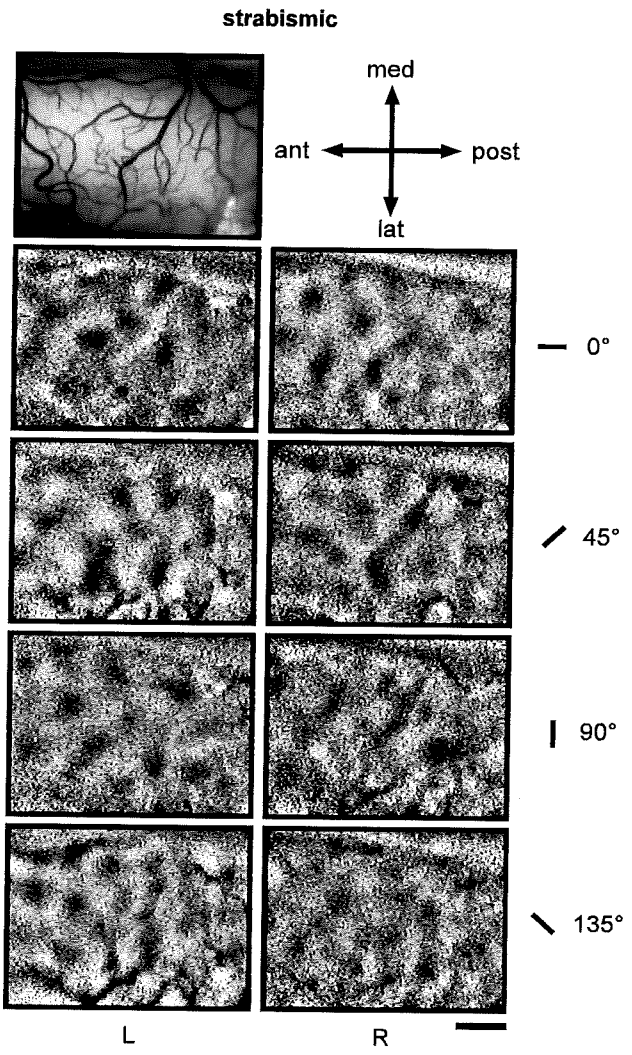

Fig. 3. Monocular iso-orientation domains in the left area 17 of a convergently squinting cat (S1). Blood vessel pattern of the imaged cortical area (4.8 × 3.6 mm) at top left. Cortical activation patterns were visualized by optical imaging of intrinsic signals while the animal was stimulated through the left (L, left column) and right eye (R, right column) with oriented gratings of 0, 45, 90, and 135 deg. Note that the patterns were clearly different for left and right eye stimulation. Abbreviations: ant: anterior; lat: lateral; post: posterior; and med: medial. Scale bar = 1 mm.

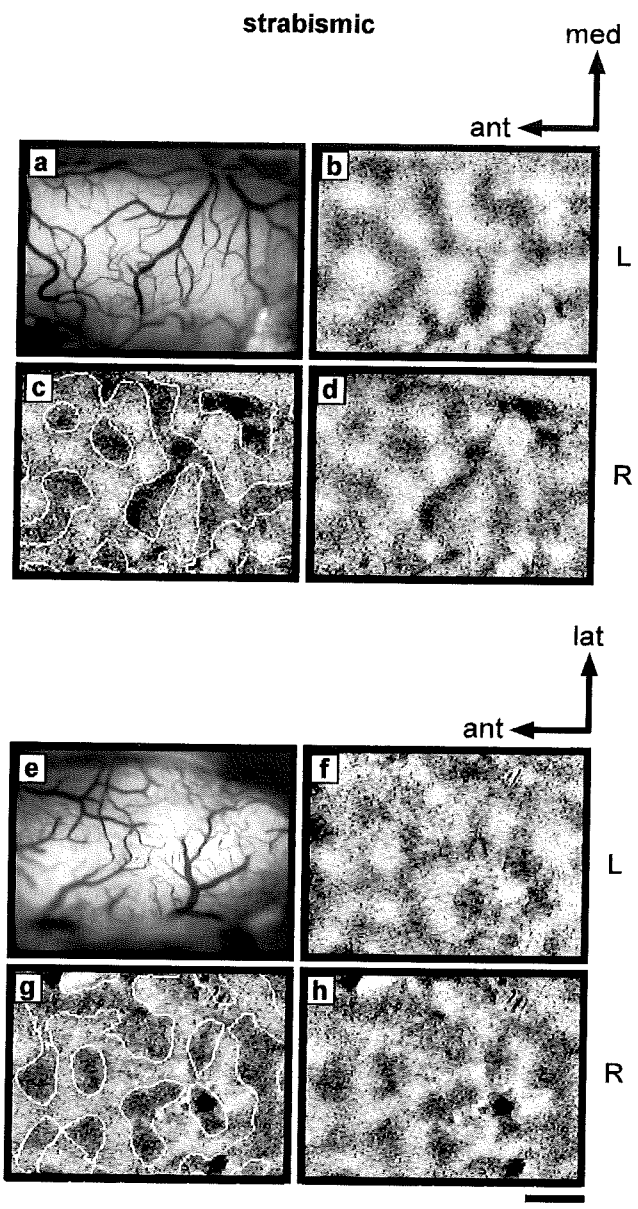

Fig. 4. Ocular dominance domains in area 17 of two convergently squinting (esotropic) cats. The blood vessel pictures of the imaged cortical areas are illustrated in (a) and (e). Optically visualized ocular dominance domains in the left area 17 of cat S1 (b–d) and in the right area 17 of cat S6 (f–h). Cortical activation patterns for the nondeviating (left = L) eye are displayed in (b) and (f), those for the deviating (right = R) eye in (d) and (h). In (c) and (g), the domains of the right eyes are outlined in white. Note that activation patterns for the left and right eyes are rather complementary [compare (b) with (d) and (f) with (h)]: regions heavily activated by the left eye [dark regions in (b) and (f)] are only weakly activated by the right eye [light grey regions in (d) and (h)]. Abbreviations are as in Fig. 3. Scale bar = 1 mm.

To further characterize the layout of the functional domains, we determined the spatial density of the pinwheel centers. An example is shown in Fig. 7d for the angle map of Fig. 7c. To this end, we performed a semiautomatic analysis of angle maps as previously published (Löwel et al., 1998) and briefly described in the Materials and methods. Individual pinwheel densities are presented in Table 2. The average pinwheel density (± 1 SEM) was 3.4 ± 0.1 pinwheels per mm^2 (range 3.2–3.8) cortical surface in strabismic cats (7 hemispheres) and 3.4 ± 0.03/mm^2 (range 3.3–3.4) cortical surface in normally raised control animals (3 hemispheres). Thus, pinwheel density was essentially the same in convergently squinting and control cats of our colony ($P > 0.1$; t-test). These absolute values were, however, higher than those previously reported for normal (Rao et al., 1997: 2.4/mm^2; Bonhoeffer et al., 1995: 2.1/mm^2; Löwel et al., 1998: 2.6/mm^2 cortical surface) and divergently squinting cats (Löwel et al., 1998: 2.7/mm^2 cortical surface). Statistical analysis revealed a highly significant difference in pinwheel densities between animals of the present study ($n = 10$ hemispheres; Magdeburg colony) and those previously analyzed ($n = 10$ hemispheres; Frankfurt colony; Löwel et al., 1998) ($P < 0.00001$, t-test).

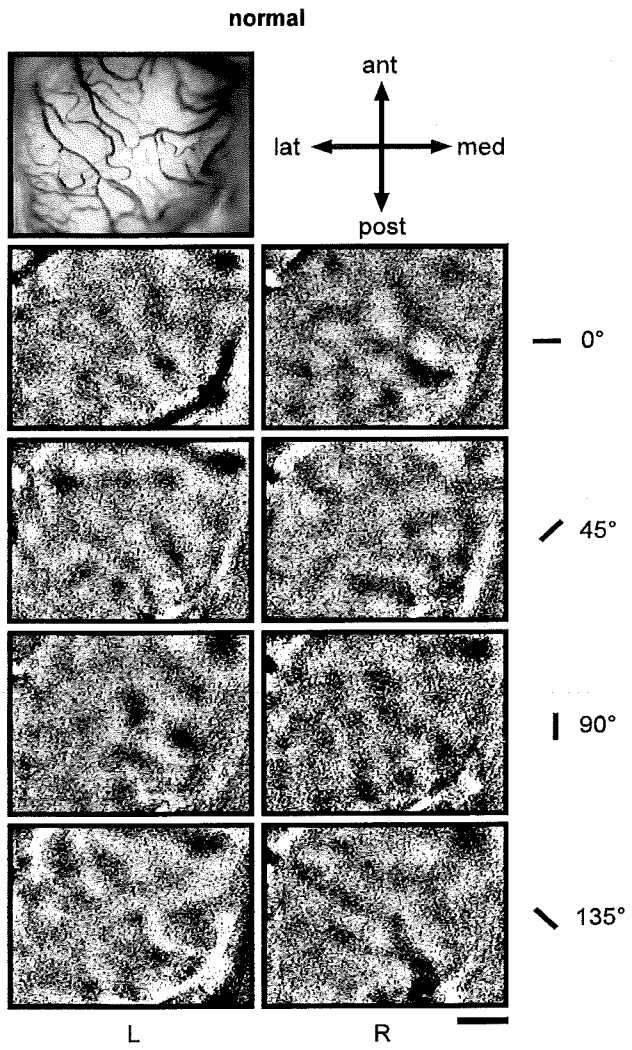

Fig. 5. Monocular iso-orientation domains in the left area 17 of a normal cat (N1). Blood vessel pattern of the imaged cortical area (4.8 × 3.6 mm) at top left. Cortical activation patterns were visualized by optical imaging of intrinsic signals while the animals were stimulated through the left (L, left column) or right eye (R, right column) with oriented gratings of 0, 45, 90, and 135 deg. Note that activity maps were rather similar after left and right eye stimulation (compare left and right columns). Abbreviations are as in Fig. 3. Scale bar = 1 mm.

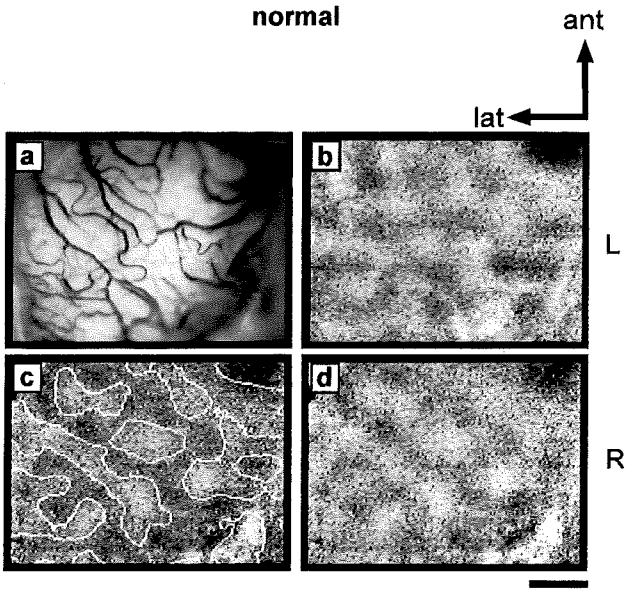

Fig. 6. Ocular dominance domains in the left area 17 of a normally raised control cat (N1). (a) Blood vessel pattern of the imaged cortical area. Cortical activation pattern for the left (L, b) and right (R, d) eye. The white contours in (c) delineate the right eye domains. Note that the ocular-dominance domains are less clearly segregated (i.e. the contrast is weaker) compared with the squinting animals. Abbreviations are as in Fig. 3. Scale bar = 1 mm.

Topographic relationship between ocular dominance and iso-orientation domains

Intersection angles

Comparisons of orientation and ocular dominance maps in the convergently squinting cats revealed that iso-orientation domains were continuous across the borders of ocular dominance domains (Figs. 7e & 7f). A similar topographic relationship has been described previously for both normally raised (Hübener et al., 1997) and divergently squinting cats (Löwel et al., 1998). To analyze this continuity quantitatively, we determined the angle of intersection between orientation and ocular dominance domains in all the optically imaged functional maps. Iso-orientation contours tended to intersect the borders of adjacent ocular dominance do-mains at steep angles (Fig. 7f). Fig. 8 shows histograms of intersection angles in three convergently squinting cats, revealing a preponderance of angles between 75 and 90 deg. In these typical cases, between 22 and 24% of all intersection angles fell within this range (Fig. 8, left column). To test for the possibility that the tendency for orthogonal intersections was merely an accidental feature, we redetermined intersection angles after shifting the two maps from the same animal (Fig. 8, right column). In each case, the distribution of intersection angles was rather flat. These data indicate that iso-orientation and ocular dominance domains are not independent but exhibit a systematic topographic relationship as was originally suggested by Hubel and Wiesel (1977) on the basis of electrophysiological recordings.

Localization of pinwheel centers

In normally raised kittens, pinwheel singularities have been reported to lie preferentially in the centers of ocular dominance domains (Crair et al., 1997*a*,*b*; Hübener et al., 1997; see also Matsuda et al., 2000). However, in previous analyzes from divergently squinting cats this tendency was, although present, not statistically significant (Löwel et al., 1998). Quantitative analyzes of pinwheel localizations in convergently squinting cats revealed that there was only a weak tendency for pinwheel centers to lie in the center of ocular dominance domains and to avoid ocular-dominance borders (Fig. 9). This tendency was present only for singularities of the ipsilateral eye, as reported previously for kitten area 17 (Matsuda et al., 2000), but it was not statistically significant ($n = 4$, Fig. 9) ($P > 0.1$; chi-square test). Thus, orientation pinwheel centers in convergently squinting cats did not exhibit a consistent and significant topographical relationship to the peaks of ocular dominance domains.

Discussion

The main results of the present study are as follows: (1) The functional architecture of area 17 of convergently squinting cats—as

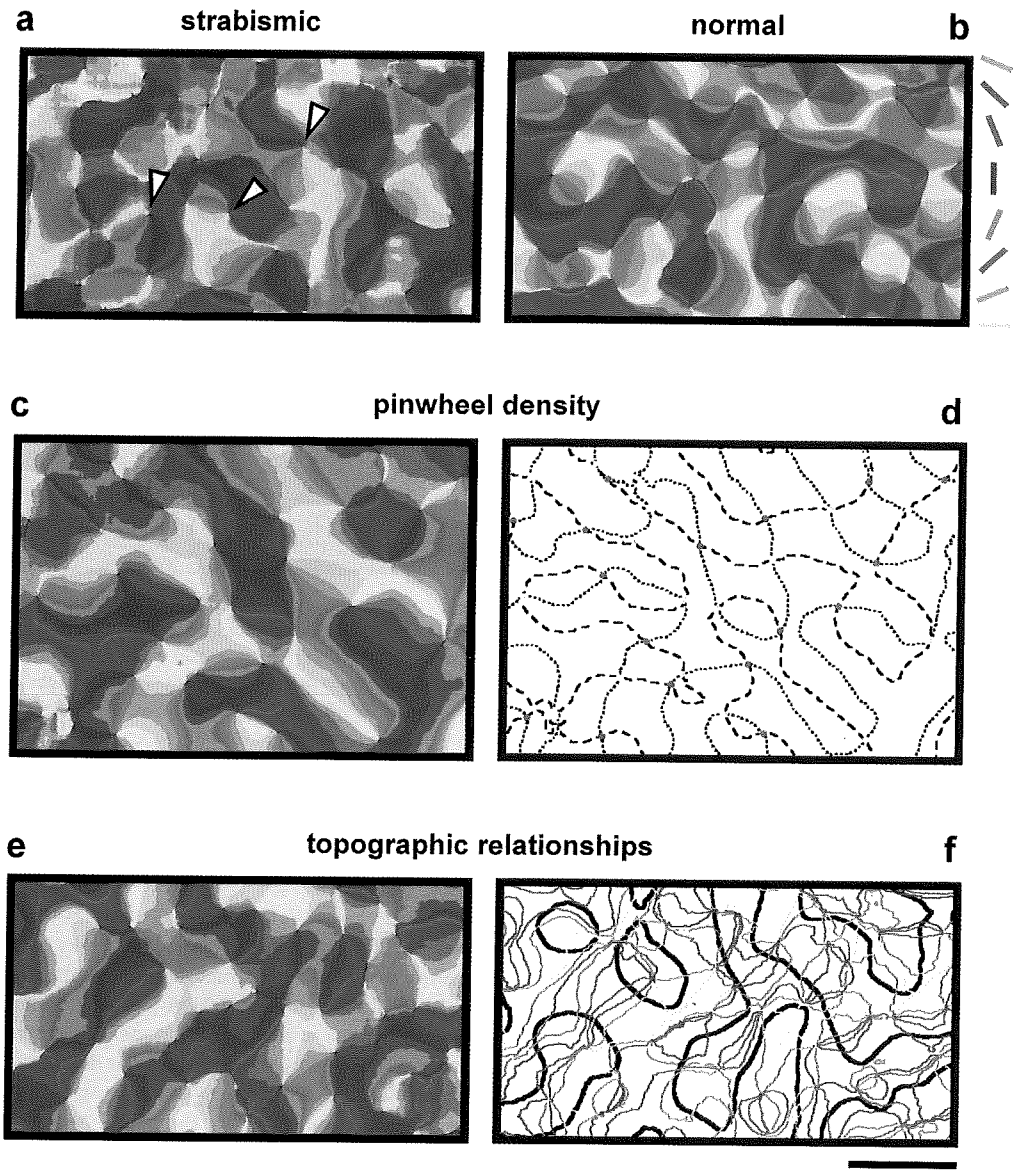

Fig. 7. Orientation preference ("angle") maps and their quantitative and topographic analysis in area 17 of convergently squinting (a, e, f) and normally raised control cats (b, c, d). In the angle maps, the preferred orientation for every region of the imaged cortex is color coded according to the scheme in (b). (a–c, e) Angle maps from the right and left area 17 of esotropic cats S2 (a) and S1 (e) and from the left hemispheres of the normally raised control animals N2 (b) and N1 (c). Note the pinwheel-like organization of orientation domains in both esotropic and normal control cats: there are numerous pinwheel center singularities in the map around which all colors (orientations) appear once [see arrowheads in (a)]. (c, d) Quantitative analysis of the distribution and spatial density of orientation (pinwheel) centers. The angle map of the analyzed cortical region (c) was 9.7 mm^2 in size. Locations of pinwheel centers corresponding to the crossings of the dotted with the broken lines (d) (the 0 deg/90 deg and the 45 deg/135 deg orientation contours). Red respectively yellow dots correspond to pinwheel centers of opposite chirality (red: +1/2, yellow: −1/2). The illustrated angle map contains 33 pinwheel centers corresponding to a pinwheel density of 3.4/mm^2 cortical surface. (e, f) Topographic relationship between iso-orientation and ocular dominance columns in cat S1. Superposition of iso-orientation contours (colored lines) and the outlined borders of ocular dominance columns (black lines; see also Fig. 4). Note that domains of like orientation preference labelled by the same color in the angle map are continuous across the borders of ocular dominance domains (f). Scale bar = 1 mm.

assessed by intrinsic signal imaging—is similar to that described previously for divergently squinting cats (Löwel et al., 1998). (2) Convergently squinting and normally raised control cats are similar with respect to (i) intersection angles of iso-orientation and ocular-dominance domains and (ii) pinwheel densities in orientation preference maps. (3) Pinwheel center location seems to be more heterogeneous than in normally raised animals: Although there is a tendency for pinwheel centers to avoid the borders of ocular-dominance domains and to be located in the centers of ipsilateral eye domains, this tendency is not statistically significant in cats with convergent strabismus. (4) Compared with previous studies in divergently squinting and normally raised cats, we observed a significantly higher pinwheel density in orientation-preference maps in area 17 of both experimental and control animals.

The similarity in the functional organization of orientation and ocular dominance domains in area 17 of convergently and diver-

Table 2. *Pinwheel densities in area 17 of esotropic (S1–S5) and normally raised cats (N1–N2)*[a]

Cat/ Hemisphere	Age (months)	Pinwheel density (1/mm^2)	Cortical area (mm^2)
S1, LH	13	3.3	10.2
S1, RH	13	3.7	9.9
S2, LH	14	3.6	10.8
S2, RH	14	3.3	9.5
S3, LH	8	3.2	8.6
S4, RH	13	3.2	9.0
S5, RH	11	3.8	8.7
N1, LH	39	3.4	9.7
N2, LH	6	3.4	8.3
N2, RH	6	3.3	9.3

[a]LH: left hemisphere; RH: right hemisphere. Age: age at the time of optical imaging. Pinwheel density (1/mm^2): density of pinwheel centers per mm^2 cortical surface. Cortical area (mm^2): size of the cortical area used for quantitative analyzes of pinwheel densities.

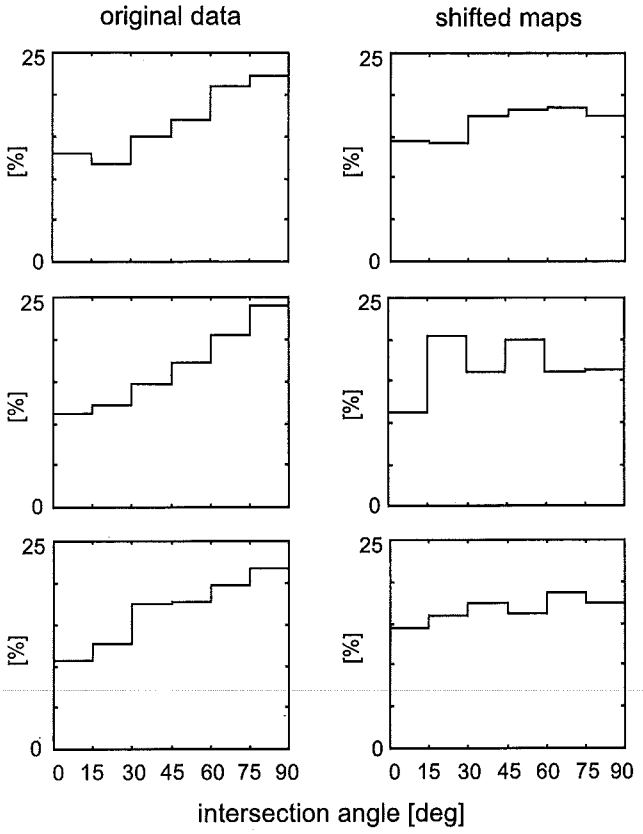

Fig. 8. Histograms of intersection angles between iso-orientation and ocular-dominance columns in convergently squinting cats (S1, S2, S3; from top to bottom). *X*-axis, intersection angle in degrees from 0 deg to 90 deg divided into six classes (0–15 deg, 15–30 deg, ... 75–90 deg). *Y*-axis, percentage of intersection angles in each class. Left column, original data; right column, "shifted" maps: histograms after shifting the maps against each other. Note that intersection angles between 75 deg and 90 deg are most abundant in the original data of all cases; also that the histograms are rather flat after shifting the maps.

gently squinting cats is not self-evident. In convergent squinters, the optical axis of the eyes cross, resulting in complex left/right relationships which conceivably induce compensation strategies that are quite different from those employed in divergent squinters. The similarity in the layout of orientation and ocular dominance maps in esotropic and exotropic cats therefore suggests that a similar strategy to avoid double vision corresponds with a similar functional organization of the primary visual cortex.

As previously described for cats with divergent strabismus (Löwel & Singer, 1993; Löwel et al., 1998), the cortical activity patterns induced by left or right eye stimulation were rather complementary so that clearly segregated ocular dominance domains could be visualized. This is in contrast to the situation in our normally raised control cats, in which monocular orientation maps were much more similar. Both observations fit perfectly with the known electrophysiological properties of visual cortical neurons: in strabismics, neurons are driven rather exclusively by stimulation of either the left or the right eye whereas in normally raised animals, the vast majority of neurons are binocularly driven (Hubel & Wiesel, 1965). Interestingly, ocular dominance domains can easily be visualized in normally raised kittens (Hübener et al., 1997; Crair et al., 1997*a*, 1998) which might indicate that the optical signal recorded in very young animals is dominated by neuronal activity in the input layer IV of primary visual cortex which contains the highest proportion of monocularly driven neurons (Albus, 1975; for review see Frégnac & Imbert, 1984).

In contrast to the differences of the ocular dominance system in normal and strabismic cats, orientation-preference maps do not display any obvious experience-dependent changes. As previously described for normally raised (Bonhoeffer et al., 1995; Crair et al., 1997*a*,*b*; 1998; Hübener et al., 1997) and divergently squinting cats (Löwel et al., 1998), convergently squinting cats also show a pinwheel-like organization of iso-orientation domains in area 17. Quantitative analysis of orientation-preference maps revealed that the average pinwheel density was similar for normal and convergently squinting cats. However, there seems to exist a general population difference because the absolute pinwheel densities for both groups of animals in the present study (3.4 pinwheels /mm^2) were significantly higher than the pinwheel densities reported previously for normally raised (Rao et al., 1997: 2.4/mm^2; Bonhoeffer et al., 1995: 2.1/mm^2; Löwel et al., 1998: 2.6/mm^2 cortical surface) and divergently squinting cats (Löwel et al., 1998: 2.7/mm^2 cortical surface). One possible explanation for this observation is that genetic factors influence quantitative features of functional cortical maps. This hypothesis is supported by the recent observation that orientation column sizes and shapes as well as a measure of the homogeneity of column sizes across area 17 are indeed significantly more similar in genetically related animals and in the two hemispheres of individual brains compared with the overall interindividual variability (Löwel et al., 2000).

The iso-orientation domains of the convergent squinters were continuous across the borders of ocular dominance domains. Furthermore iso-orientation contours tended to intersect the borders of adjacent ocular dominance domains at steep angles, as previously described for both normally raised (e.g. Hübener et al., 1997) and divergently squinting cats (Löwel et al., 1998). The most likely explanation for this scenario is that the basic layout of orientation-preference maps is already specified before ocular dominance maps develop, supporting the notion that the selection of thalamic input connections is guided by the already existing orientation map. This possibility is supported by a number of observations,

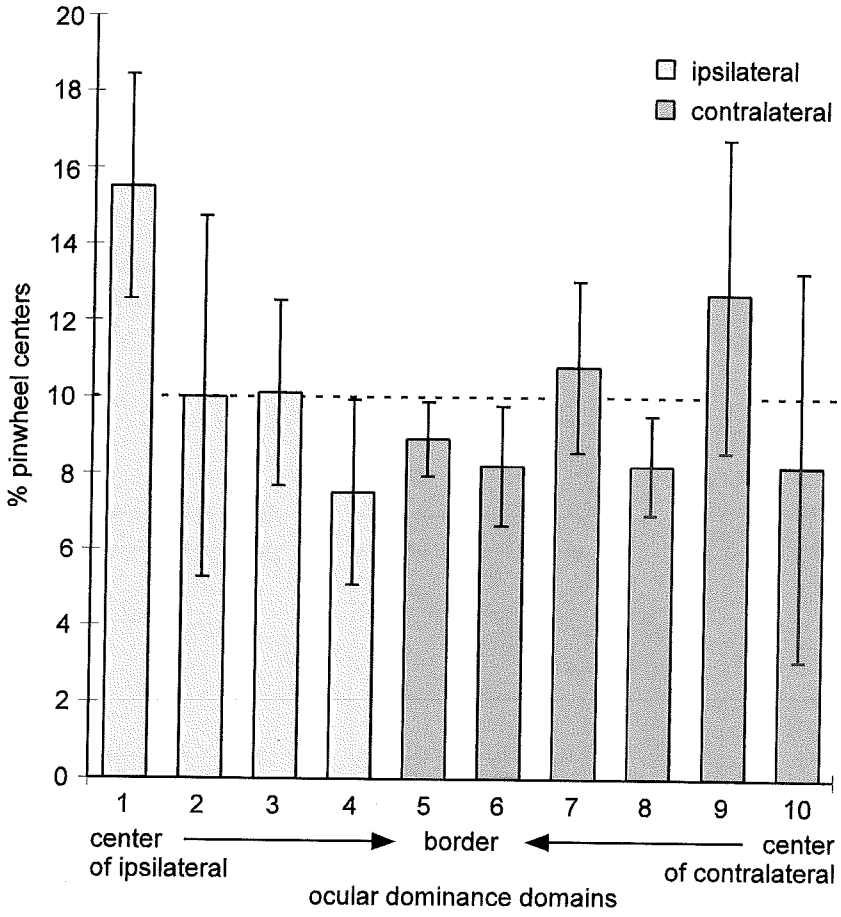

Fig. 9. Relative frequency of pinwheel centers in subregions of contralateral and ipsilateral eye domains. The maps (n = 4) were divided into ten regions of equal area, with the 0–10 and 90–100 percentile corresponding to the peak of the ipsilateral (class 1) and contralateral (class 10) eye domains, and the 40–50 and 50–60 percentile corresponding to the border regions of the ocular-dominance domains (classes 5 and 6). Error bars represent 1 SEM. The dashed line indicates the expected value (10%) if the pinwheel centers were distributed randomly. Note that the locations of the pinwheel centers were quite variable, although there was a weak tendency for the pinwheel centers of the ipsilateral eye to be preferentially located in the center regions of the ocular dominance domains. This tendency was, however, not statistically significant.

including the demonstration of orientation-selective neurons in kittens before eye opening (Hubel & Wiesel, 1963) and the visualization of well-organized maps of orientation preference already in 2-week-old kittens (Crair et al., 1998; for further discussion see Löwel et al., 1998).

The observation of a largely unchanged geometrical relationship between ocular dominance and iso-orientation domains in strabismic compared with normally raised cats further suggests that this particular geometrical arrangement is advantageous for cortical organization (Kim et al., 1999; Koulakov & Chklovskii, 2001) and should therefore not be modified by visual experience. Indeed, it has recently been shown that the topographical relationships of visual cortical maps are optimized for uniform coverage (Swindale et al., 2000). When the spatial relationships between ocular dominance, spatial frequency, and orientation maps recorded simultaneously from selected regions of the visual cortex were perturbed by either shifting or mirror inversing, coverage uniformity values got worse, indicating that cortical maps are at a local minimum for coverage uniformity (Swindale et al., 2000).

Recently, another specific geometrical relationship between orientation and ocular dominance domains was described for cat area 17. Detailed analysis of optically recorded functional maps in 8–12 weeks old cats revealed that orientation pinwheel centers coincide with ipsilateral, but not with contralateral ocular dominance domains (Matsuda et al., 2000; see also Crair et al., 1997*a*,*b*; Hübener et al., 1997). Our analysis in esotropic cats did, however, not reveal a statistically significant geometrical relationship between pinwheel centers and the peaks of ocular dominance domains, in accordance with a recent analysis in exotropic cats (Löwel et al., 1998). We therefore suggest that the pronounced monocularity of squinters might weaken the constraints on pinwheel location so that the distribution of pinwheel centers with respect to ocular dominance domains is more heterogeneous in strabismic (both esotropic and exotropic) than in normally raised cats.

Conclusions

1. Our observations indicate a general similarity between the layout of orientation and ocular dominance maps in area 17 of convergently (nonamblyopic) and divergently squinting cats. This suggests that the strategy to avoid double vision (alternation or suppression), and not squint angle *per se*, might influence the functional organization of primary visual cortex.
2. The pronounced monocularity of squinters might weaken the constraints on pinwheel location so that the distribution of pinwheel centers with respect to ocular dominance domains is more heterogeneous in strabismic than in normally raised cats.
3. The higher pinwheel densities in the orientation-preference maps of both experimental and control cats compared with those reported for normally raised and divergently squinting cats indicates that genetic factors may influence quantitative parameters of functional cortical maps.

Acknowledgments

We would like to thank Fred Wolf, Frank Hoffsümmer, and Michael Schnabel for there invaluable help with image analyzes. Special thanks are due to Stefan Rathjen, Steffi Bachmann, and Susann Becker for their assistance with the behavioral training and testing of the cats, and to Ruxandra Sireteanu and Pieter Roelfsema for sharing with us their knowledge of cat psychophysics. This work was supported by DFG Grant LO442/5-1 and LO 442/5-2, and by the WGL.

References

ALBUS, K. (1975). Predominance of monocularity driven cells in the projection area of the central visual field in cat's striate cortex. *Brain Research* **89**, 341–347.

BLAKEMORE, C. (1976). The conditions required for the maintenance of binocularity in the kitten's visual cortex. *Journal of Physiology* **261**, 423–444.

BLASDEL, G.G. & SALAMA, G. (1986). Voltage sensitive dyes reveal a modular organization in monkey striate cortex. *Nature* **321**, 579–585.

BONHOEFFER, T. & GRINVALD, A. (1993). The layout of iso-orientation domains in area 18 of cat visual cortex: Optical imaging reveals a pinwheel-like organization. *Journal of Neuroscience* **13**, 4157–4180.

BONHOEFFER, T., KIM, D.S., MALONEK, D., SHOHAM, D. & GRINVALD, A. (1995). Optical imaging of the layout of functional domains in area 17 and across the area 17/18 border in cat visual cortex. *European Journal of Neuroscience* **7**, 1973–1988.

BONHOEFFER, T. & GRINVALD, A. (1996). Optical imaging based on intrinsic signals: The methodology. In *Brain mapping: The methods*, ed. TOGA, A. & MAZZIOTTA, J.C., pp. 55–97. San Diego, California: Academic Press.

CLELAND, B.G., CREWTHER, D.P., CREWTHER, S.G. & MITCHELL, D.E. (1982). Normality of spatial resolution of retinal ganglion cells in cats with strabismic amblyopia. *Journal of Physiology* **326**, 235–249.

CRAIR, M.C., RUTHAZER, E.S., GILLESPIE, D.C. & STRYKER, M.P. (1997*a*). Relationship between the ocular dominance and orientation maps in visual cortex of monocularly deprived cats. *Neuron* **19**, 307–318.

CRAIR, M.C., RUTHAZER, E.S., GILLESPIE, D.C. & STRYKER, M.P. (1997*b*). Ocular dominance peaks at pinwheel center singularities of the orientation map in cat visual cortex. *Journal of Neurophysiology* **77**, 3381–3385.

CRAIR, M.C., GILLESPIE, D.C. & STRYKER, M.P. (1998). The role of visual experience in the development of columns in cat visual cortex. *Science* **279**, 566–570.

CREWTHER, S.G., CREWTHER, D.P. & CLELAND, B.G. (1985). Convergent strabismic amblyopia in cats. *Experimental Brain Research* **60**, 1–9.

DUKE-ELDER, S. & WYBAR, K. (1973). *System of Ophthalmology. VI. Ocular Motility and Strabismus*. London: Kimpton.

ENGELMANN, R., CROOK, J.M., & LÖWEL, S. (1999). Optical imaging of orientation and ocular dominance maps in area 17 of convergently squinting cats. *Society for Neuroscience Abstracts* **25**, 572.14.

FRÉGNAC, Y. & IMBERT, M. (1984). Development of neuronal selectivity in the primary visual cortex of the cat. *Physiological Reviews* **64**, 325–434.

GRANT, S. & BERMAN, N.E. (1991). Mechanism of anomalous retinal correspondence: Maintenance of binocularity with alteration of receptive-field position in the lateral suprasylvian (LS) visual area of strabismic cats. *Visual Neuroscience* **7**, 259–281.

GRINVALD, A., LIEKE, E., FROSTIG, R.D., GILBERT, C.D. & WIESEL, T.N. (1986). Functional architecture of cortex revealed by optical imaging of intrinsic signals. *Nature* **324**, 361–364.

HUBEL, D.H. & WIESEL, T.D. (1963). Receptive fields of cells in striate cortex of very young, visually inexperienced kittens. *Journal of Neurophysiology* **26**, 994–1002.

HUBEL, D.H. & WIESEL, T.N. (1965). Binocular interaction in striate cortex of kittens reared with artificial squint. *Journal of Neurophysiology* **28**, 1041–1059.

HUBEL, D.H. & WIESEL, T.N. (1977). Ferrier lecture. Functional architecture of macaque monkey visual cortex. *Proceedings of the Royal Society B* (London) **198**, 1–59.

HÜBENER, M., SHOHAM, D., GRINVALD, A. & BONHOEFFER, T. (1997). Spatial relationships among three columnar systems in cat area 17. *Journal of Neuroscience* **17**, 9270–9284.

KALIL, R.E., SPEAR, P.D. & LANGSETMO, A. (1984). Response properties of striate cortex neurons in cats raised with divergent or convergent strabismus. *Journal of Neurophysiology* **52**, 514–537.

KATZ, B. & SIRETEANU, R. (1992). Development of visual acuity in kittens: A comparison between jumping stand and Teller acuity card test. *Clinical Vision Science* **7**, 219–224.

KIM, D.S., MATSUDA, Y., OHKI, K., AJIMA, A. & TANAKA, S. (1999). Geometrical and topological relationships between multiple functional maps in cat primary visual cortex. *Neuroreport* **10**, 2515–2522.

KÖNIG, P., ENGEL, A.K., LÖWEL, S. & SINGER, W. (1993). Squint affects synchronization of oscillatory responses in cat visual cortex. *European Journal of Neuroscience* **5**, 501–508.

KOULAKOV, A.A. & CHKLOVSKII, D.B. (2001). Orientation preference patterns in mammalian visual cortex: A wire length minimization approach. *Neuron* **29**, 519–527.

LÖWEL, S. & SINGER, W. (1992). Selection of intrinsic horizontal connections in the visual cortex by correlated neuronal activity. *Science* **255**, 209–212.

LÖWEL, S. & SINGER, W. (1993). Monocularly induced 2-deoxyglucose patterns in the visual cortex and lateral geniculate nucleus of the cat: II. Awake animals and strabismic animals. *European Journal of Neuroscience* **5**, 857–869.

LÖWEL, S. (1994). Ocular dominance column development: Strabismus changes the spacing of adjacent columns in cat visual cortex. *Journal of Neuroscience* **14**, 7451–7468.

LÖWEL, S., SCHMIDT, K.E., KIM, D.S., WOLF, F., HOFFSÜMMER, F., SINGER, W. & BONHOEFFER, T. (1998). The layout of orientation and ocular dominance domains in area 17 of strabismic cats. *European Journal of Neuroscience* **10**, 2629–2643.

LÖWEL, S., KASCHUBE, M., GEISEL, T. & WOLF, F. (2000). Substantial genetic influence on visual cortical orientation maps. *Society for Neuroscience Abstracts* **26**, 309.1.

MAFFEI, L. & BISTI, S. (1976). Binocular interaction in strabismic kittens deprived of vision. *Science* **191**, 579–580.

MATSUDA, Y., OHKI, K., SAITO, T., AJIMA, A. & KIM, D.S. (2000). Coincidence of ipsilateral ocular dominance peaks with orientation pinwheel centers in cat visual cortex. *Neuroreport* **11**, 3337–3343.

MILLERET, C. & HOUZEL, J.C. (2001). Visual interhemispheric transfer to areas 17 and 18 in cats with convergent strabismus. *European Journal of Neuroscience* **13**, 137–152.

MITCHELL, D.E., GIFFIN, F., WILKINSON, F., ANDERSON, P. & SMITH, M.L. (1976). Visual resolution in young kittens. *Vision Research* **16**, 363–366.

OLSON, C.R. & FREEMAN, R.D. (1978). Eye alignment in kittens. *Journal of Neurophysiology* **41**, 848–859.

RAO, S.C., TOTH, L.J. & SUR, M. (1997). Optically imaged maps of orientation preference in primary visual cortex of cats and ferrets. *Journal of Comparative Neurology* **387**, 358–370.

ROELFSEMA, P.R., KÖNIG, P., ENGEL, A.K., SIRETEANU, R. & SINGER, W. (1994). Reduced synchronization in the visual cortex of cats with strabismic amblyopia. *European Journal of Neuroscience* **6**, 1645–1655.

SHATZ, C.J., LINDSTRÖM, S. & WIESEL, T.N. (1977). The distribution of afferents representing the right and left eyes in the cat's visual cortex. *Brain Research* **131**, 103–116.

SHERMAN, S.M. (1972). Development of interocular alignment in cats. *Brain Research* **37**, 187–203.

SIRETEANU, R., SINGER, W., FRONIUS, M., GREUEL, J.M., BEST, J., FIORENTINI, A., BISTI, S., SCHIAVI, C. & CAMPOS, E. (1993). Eye alignment and cortical binocularity in strabismic kittens: A comparison between tenotomy and recession. *Visual Neuroscience* **10**, 541–549.

SWINDALE, N.V., SHOHAM, D., GRINVALD, A., BONHOEFFER, T. & HÜBENER, M. (2000). Visual cortex maps are optimized for uniform coverage. *Nature Neuroscience* **3**, 822–826.

TIEMAN, S.B. & TUMOSA, N. (1997). Alternating monocular exposure increases the spacing of ocularity domains in area 17 of cats. *Visual Neuroscience* **14**, 929–938.

VON GRÜNAU, M.W. (1979). The role of maturation and visual experience in the development of eye alignment in cats. *Experimental Brain Research* **37**, 41–47.

VON GRÜNAU, M.W. & RAUSCHECKER, J.P. (1983). Natural strabismus in non-Siamese cats: Lack of binocularity in the striate cortex. *Experimental Brain Research* **52**, 307–310.

VON NOORDEN, G.K. (1990). *Binocular Vision and Ocular Motility. Theory and Management of Strabismus*. St. Louis, MO: C.V. Mosby Co.

YIN, Z.Q., LI, C.Y., PEI, X., VAEGAN, & FANG, Q.X. (1994). Development of pattern ERG and pattern VEP spatial resolution in kittens with unilateral esotropia. *Investigative Ophthalmology and Visual Science* **35**, 626–634.